Supporting Information

Popova et al. 10.1073/pnas.0906546107

SI Text

SI Results ***Growth of the phoΔnull strain is supported only by Gly3P and GlyPIno as the sole source of phosphate.*** We have tested which phosphate-containing compounds or analogues could be used as the sole source of phosphate by the *phoΔnull* strain (*pho84*Δ *pho87*Δ *pho89*Δ *pho90*Δ *pho91*Δ). This strain lacks all phosphate carriers and is therefore completely deficient in phosphate uptake. It can also not utilize any phosphate derived from extracellular hydrolysis of phosphate-containing compounds. The results show that this strain can grow only in the presence of Gly3P or GlyPIno, which are transported by Git1, and not in the presence of any other compound tested (Fig. S1). The other compounds are either not transported or the cells lack a phosphatase that can release free phosphate from the compound. For the metabolic intermediates, absence of transport is the most likely explanation.

Activation by organic phosphate compounds is not due to contaminating phosphate. We have performed multiple control experiments to rule out alternative explanations for the agonist action of Gly3P and the other organic phosphate esters. We eliminated the possibility that contaminating phosphate in the commercial preparations would be responsible for the activation. For that purpose, we first measured phosphate in all commercial preparations used. The level of phosphate detected was very low: less than 20 μM. Control experiments showed that this level of phosphate was able to trigger only a very small, short-lived activation and not able to trigger the sustained activation observed with Gly3P and the other organic phosphate compounds.

To exclude the remote possibility that this very low level of phosphate was still involved in some way in the activation, we have removed this phosphate by preincubation with cells. For that purpose, we used cells of the *git1*Δ *pho91*Δ strain because they are able to take up phosphate but not Gly3P. We carried out a first trehalase activation experiment with *git1*Δ *pho91*Δ *pho3*Δ *pho5*Δ cells, in which we incubated the cells for 2 hours with either 0.2 mM phosphate or with 10 mM Gly3P and measured trehalase activation in the usual way. Subsequently, the cells were removed from the suspension by centrifugation and discarded. The supernatant was then added to fresh cells, and we determined whether it could trigger a second activation of trehalase. Fig. S2 shows that only with the cells preincubated with Gly3P was a second activation observed, whereas with the cells preincubated with 0.2 mM phosphate, no second activation was observed. This indicates that the cells could take up in this time period all the phosphate from the medium so that no second phosphate-induced activation could took place anymore. As opposed to phosphate, the second activation with Gly3P was still clearly present, eliminating the possibility that phosphate present in the Gly3P preparation and not the Gly3P itself is responsible for trehalase activation.

Activation by organic phosphate compounds is not due to residual secreted phosphatase activity. Pho3 and Pho5 are the main secreted phosphatases in yeast (1). They are responsible for nearly all extracellular phosphatase activity. To rule out that any residual secreted phosphatase activity was involved in the activation by Gly3P, we first measured the free phosphate level in the medium of a *pho3*Δ *pho5*Δ cell suspension incubated with Gly3P or GlyPIno over the same time period as used to measure trehalase activation. We could not detect any significant level of phosphate produced in the medium. To completely exclude the remote possibility that very low secreted activity of other phosphatases would be involved, we constructed a quadruple deletion strain lacking two other, possibly secreted phosphatases: *pho3*Δ *pho5*Δ *pho11*Δ *pho12*Δ. With this strain, however, we observed the same extent of trehalase activation as with the wild-type and *pho3*Δ *pho5*Δ strains, for all compounds tested (Fig. S3). This supports our conclusion that activation of the protein kinase A (PKA) pathway by Gly3P and the other organic phosphate compounds is truly because of interaction of these compounds with Pho84 and not because of activation by phosphate generated extracellularly by secreted phosphatase activity during the experiment.

Gly3P-induced trehalose mobilization is supported only by Pho84. We have investigated Gly3P-induced trehalose mobilization in a *pho84*Δ *pho87*Δ *pho89*Δ *pho90*Δ *pho91*Δ *(phoΔnull) git1*Δ strain with overexpression of one of the following carriers: *PHO84*, *PHO87*, *PHO89*, *PHO90*, *PHO91*, or *GIT1*. The results show that overexpression of *PHO84* leads to a lower initial trehalose content and that only expression of *PHO84* is able to support Gly3P-induced trehalose mobilization (Fig. S4). This is consistent with the results obtained for Gly3P-induced trehalase activation shown in Fig. 1*C* of the main text. The higher basal trehalase activity in the strain with overexpression of *PHO84* fits with the lower basal trehalose content, and only this strain was able to support Gly3P-induced trehalase activation.

Phosphate and Gly3P affect other targets in a similar, PKA-dependent manner. We have also measured the response of other targets of the PKA pathway to addition of phosphate and Gly3P in a wild-type strain and a strain with reduced activity of PKA (*tpk1*Δ *tpk2*Δ *TPK3*). Determination of repression of the Stress Response Element (STRE)-controlled gene *SSA3* showed a similar response to phosphate and Gly3P in wild-type cells and a reduced response in the *tpk1*Δ *tpk2*Δ *TPK3* strain (Fig. S5*A*). We also performed microarray analysis of genome-wide gene expression with phosphate-starved cells as control and phosphate-starved cells to which phosphate or Gly3P was added for 60 min. This was done with the wild-type strain and with a strain with reduced PKA activity (*tpk1*Δ *tpk2*Δ *TPK3*). The results show that the genome-wide transcription response of the wild-type cells to phosphate and Gly3P is strikingly similar. In the strain with the reduced PKA activity the response to the two compounds is still similar but clearly much less than in the wild-type strain (Fig. S5*B*). This confirms that phosphate and Gly3P have a very similar effect on wild-type cells and that activation of the PKA pathway plays a major role in the common response. When the PKA activity is artificially reduced, other pathways and interactions apparently start having effect. These effects are superseded by full PKA pathway activation in the wild-type cells.

Gly3P is transported by Git1 and Pho91 but not by Pho84, as determined by growth recovery of phosphate-starved cells and the increase in intracellular phosphate after supply with Gly3P. Although Pho91 was reported as being localized in the vacuolar membrane (2), deletion of the *PHO91* gene significantly reduced uptake of extracellular Gly3P (main text, Fig. 2*B*). This is consistent with at least part of Pho91 being localized in the plasma membrane, in agreement with the previously demonstrated phosphate uptake capacity of a strain expressing only Pho91 (3). We also determined growth recovery during 28 h after addition of Gly3P to phosphate-starved cells. The *pho3*Δ *pho5*Δ *pho91*Δ *git1*Δ strain showed only very slow, residual growth recovery over a time period of 28 h (Fig. S6*A*). These results confirm the importance of

Git1 and Pho91 for Gly3P uptake in phosphate-starved cells and show that none of the other carriers, including Pho84, has enough Gly3P transport activity to sustain regular growth with Gly3P as the phosphate source for a period of up to 28 h.

Measurement of the intracellular phosphate level in phosphate-limited wild-type cells or cells of the *pho3*Δ *pho5*Δ strain revealed a rapid increase after addition of Gly3P (Fig. S6*B*). In the *pho3*Δ *pho5*Δ *git1*Δ *pho91* strain the basal level of intracellular phosphate was enhanced, but there was no additional increase after addition of Gly3P (Fig. S6*B*). These results show that after uptake by Git1 and Pho91 Gly3P can be used as a source of free phosphate. They also show that the *pho3*Δ *pho5*Δ *git1*Δ *pho91* strain is unable to use Gly3P as a source of free phosphate in the first 40 min after addition.

GlyPIno activates PKA signaling through Pho84 and not via Git1-mediated transport. GlyPIno is transported by Git1 (4). Note that 0.1 and 0.5 mM GlyPIno triggered activation of PKA signaling in a *git1*Δ *pho3*Δ *pho5*Δ strain, in which it cannot be transported, but it did not trigger activation in a *pho84*Δ *pho3*Δ *pho5*Δ strain (Fig. S7). This shows that GlyPIno also triggers activation of the PKA pathway as a nontransported agonist of Pho84.

Selection of transmembrane domain (TMD) IV for substituted cysteine accessibility method (SCAM) analysis. We first selected TMD IV for SCAM analysis for the following reasons: (*i*) It contains the strongly conserved R168 residue, which may be involved in phosphate binding; (*ii*) it contains the "phosphate signature" (GGDYPLSATIXSE) found in plant phosphate transporters (5); (*iii*) it contains a sequence motif shared by proton-coupled phosphate transporters from plants, fungi, bacteria, and mammals (**T**LCFFR**F**WL**G**F**GIGGDYPLS**ATIMSE) (6); (*iv*) it contains the phosphate-binding signature sequence GXGXGG; (*v*) models of the 3D structure of Pho84 (7), *Escherichia coli* lactose permease (8) and the mammalian glucose transporter Glut1 (9, 10) predict that TMD IV may be located adjacent to the substrate passageway.

Mutagenesis of Phe^{160} to other residues similar in size as cysteine, i.e., alanine, serine, and methionine, does not result in a 2-aminoethyl methanethiosulfonate, hydrobromide (MTSEA)-sensitive allele of Pho84. The observation that mutagenesis of Phe^{160} to cysteine partially reduces transport and PKA signaling may be explained by a role of this residue in the phosphate-binding site of Pho84 but also by the mutation causing a distortion in the general conformation of the protein. Hence, a remote possibility to explain the sensitivity to MTSEA of the Pho84^{F160C} mutant protein is that in the latter case the general distortion of the protein causes abnormal exposure of the side chain of another cysteine residue located elsewhere in the protein and that binding of MTSEA to the side chain of this cysteine inactivates Pho84. To contradict this remote possibility we have mutated Phe^{160} to other residues similar in size as cysteine, i.e., alanine, serine, and methionine. All three new mutant proteins also showed to different extents a partial reduction in phosphate transport and signaling, as observed for Pho84^{F160C} (Fig. S8). None of the three mutant proteins, however, was sensitive to MTSEA (Fig. S8). We constructed GFP fusions of the new mutant proteins and showed that they are all located in the plasma membrane. These results confirm that the MTSEA sensitivity of the Pho84^{F160C} mutant protein for phosphate transport and signaling is because of the exposure of the side chain of Phe^{160} into the phosphate-binding site of Pho84.

Pho84 and orthologs in other organisms show significant sequence similarity with the Snf3 and Rgt2 glucose sensors and with Hxt glucose transporters. An alignment of TMD IV reveals several residues with complete or strong conservation in all phosphate carriers (upper series) and for part of the residues also in the Snf3 and Rgt2 glucose sensors and Hxt glucose transporters (lower series) (Fig. S9). The conservation fits well with the experimental results of TMD IV mutagenesis: All residues that are important for transport and signaling in Pho84 are either completely or strongly conserved in the other proteins.

SI Materials and Methods. ***Strains and plasmids.*** *Saccharomyces cerevisiae* strains used in this study are listed in Table S1. Plasmids EB1247, EB1368, EB1374, and EB1280 have been described previously (3).

Strain constructions. Yeast strains used in this study are shown in Table S1. Strain YP100 was constructed from the strain EY917 (3) by use of the deletion cassette, *git1::KanMX4,* generated from genomic DNA of the Y15815 strain by PCR amplification. Growth of the strain on galactose medium is supported by the p*GAL-PHO84* (EB1280) plasmid. This strain was transformed with plasmids (*URA3* marker) containing either *ADH1-GIT1* (EB1374), *ADH1-PHO84* (EB1368), *ADH1-PHO87* (EB1247), *ADH1-PHO90* (YP1314), or *ADH1-PHO91* (YP1315) constructs, and the p*GAL-PHO84* plasmid (*TRP1* marker) was lost on synthetic dextrose (SD)-ura medium. For construction of the strain YP106, the *KanMX4* marker was converted into the *LEU2* selective marker by using the "marker swap" plasmid pM4755 (11). The *PHO5* gene was inactivated by using the deletion cassette, *pho5::KanMX4,* generated from genomic DNA of the Y13232 strain by PCR amplification. Strains YP107 and YP108 were constructed from the strains EY914 and EY915, respectively (3) by use of the deletion cassette *pho5::KanMX4,* generated from genomic DNA of the Y13232 strain by PCR amplification. Strains YP109, YP110, and YP111 were obtained from strain YP108. Deletion of the *GIT1* gene in strains YP109 and YP111 was done by transformation of strain YP108 with the *git1::TRP1* PCR product, which was synthesized by using forward primer ATGGAAGACAAAGATATCACATCGGTAAATGAGAAGGAAGTGAACGAGAACACTAATCCTCAGCATCGTAATATATGTGTAC, reverse primer CTAACTTTGATCGACCTGTCTGACTGAAATTATTTCTGCGTTTTTCTGCAGGCAAGTGCACAAACAAT, and plasmid pRS314 as a template. *PHO91* deletion was introduced into strains YP110 and YP111 by transformation of strain YP108 and YP109, respectively, with a *pho91::KlURA3* PCR product, generated by using forward primer TTTATTACCCTACTTGAATTTT, reverse primer CTGGAGAACGCGTGGAACAA, and genomic DNA of strain EY918 as a template.

Plasmid constructions. Plasmids YP1314 (*PHO90*) and YP1315 (*PHO91*) were constructed by using a 5′ BamHI PCR primer TATTGGATCCATGAGATTTTCACACTTCTTGAAG (BamHI-*PHO90*) or TATTGGATCCATGAAGTTCTCGCAT (BamHI-*PHO91*) and a 3′ Not1 PCR primer TATTTGCGGCCGCTTACGCAGAGGTTGCGTTACCCTTGA (*PHO90*-NotI) or TTGCGGCCGCTTAAAATCCCATTACTTT (*PHO91*-NotI). PCR products were digested and ligated into pRS426 that contains the same *ADH1* promoter as EB1247.

Growth and phosphate starvation conditions. Cells were grown at 30 °C into exponential phase (OD_{600} = 1.0–1.5) under continuous shaking. All strains were grown in synthetic media with 2% glucose and appropriate amino acids. Strain EY917 was grown in SD containing 2% glucose with 1 g/L Gly3P (Sigma-Aldrich). Strain YP106 with constitutively overexpressed *PHO84* was cultivated in SD with 2% glucose and 1 g/L KH_2PO_4. The midexponential phase cells were harvested and transferred to phosphate starvation medium (5.7 g/L yeast nitrogen base without phosphate)

(Q-Biogene) with 4% glucose and appropriate amino acids. Cells were starved for phosphate for 3 days at 30 °C under continuous shaking, and the starvation medium was refreshed daily.

Transport assays for Gly3P and phosphate. Phosphate-starved cells were harvested and washed twice with ice-cold Mes/KOH buffer 25 mM pH 6 and resuspended in phosphate-free medium to a density of 120 mg wet weight per 1.5 mL. Aliquots of 80 μL were incubated for 15 min at 30 °C, and 20 μL Gly3P was added to a final concentration of 0.1 mM Gly3P (20,000 cpm/nmol) or 20 μL phosphate was added to a final concentration of 1 mM phosphate (10,000 cpm/nmol). After 5 min, 5 mL ice-cold water was added to stop initial transport. The cells were rapidly filtered (Whatman GF/F saturated with 0.1 mM cold Gly3P or 5 mM cold phosphate) and radioactivity on the filter was determined by liquid scintillation spectrometry. Specific transport activities are expressed as nanomole Gly3P or nanomole phosphate taken up per minute and per milligram of protein.

Biochemical determinations. For determination of trehalase activity, cells starved for phosphate for 3 days were cooled for 30 min on ice, harvested, washed twice with Mes/KOH buffer (25 mM, pH 6), and resuspended in fresh phosphate starvation medium with 4% glucose at a density of 25 mg wet weight per milliliter. Trehalase activity was determined in crude cell extracts as described previously (12). The glucose liberated was assayed by the glucose oxidase/peroxidase method. Protein was determined by the Lowry procedure. The specific activity of trehalase is expressed as nanomole glucose liberated min^{-1} $(mg\ protein)^{-1}$. For determination of intracellular phosphate, phosphate-starved cells were harvested and washed twice with ice-cold MES buffer (25 mM pH 6) and resuspended in phosphate-free medium to a density of 75 mg wet weight per milliliter. Cells were preincubated at 30 °C for 30 min. After addition of 10 mM Gly3P, samples were taken at different time points and quenched in 10 mL 60% methanol at −40 °C and centrifuged at −20 °C (5 min at 3,000 rpm). Supernatant was removed and cells were lysed in the presence of 0.5 mL perchloric acid with glass beads on a vortex. The neutralized extracts were used to determine intracellular phosphate using a standard method (13).

Q-PCR analysis. Q-PCR analysis of *SSA3* expression was carried out essentially as described previously (14). Total RNA samples were prepared by using the TRIzol reagent (Invitrogen) and treated with DNase (NEB). One microgram was used in a 20-μL reverse transcription reaction with the First Strand cDNA synthesis kit (Promega). Ten nanograms of cDNA were used in each 25-μL Q-PCR experiment. Primers were designed by using software from ABI (ABI PRISM Primer Express).

Microarray expression analysis. Total RNA was extracted by using TRIzol reagent (Invitrogen) according to the instructions of the manufacturers. Genome-wide gene expression analysis was performed by the VIB microarray service facility at the Katholieke Universiteit Leuven (Belgium). cDNA was made from the mRNA, the samples were fluorescently labeled with Cy3 or Cy5, and hybridization took place on Agilent *S. cerevisiae* microarrays (for detailed protocols, see http://www.microarrays.be/service.htm). The analysis was based on the expression values as obtained from the Agilent Feature Extraction Software version 10.5.1.1 (i.e., feature gProcessedSignal for the Cy3 signal). A quantile normalization was carried out on the log2 transformed gProcessedSignal values in order to normalize the intensities between each array.

1. Meyhack B, Bajwa W, Rudolph H, Hinnen A (1982) Two yeast acid phosphatase structural genes are the result of a tandem duplication and show different degrees of homology in their promoter and coding sequences. *EMBO J* 1:675–680.
2. Hurlimann HC, Stadler-Waibel M, Werner TP, Freimoser FM (2007) Pho91 is a vacuolar phosphate transporter that regulates phosphate and polyphosphate metabolism in Saccharomyces cerevisiae. *Mol Biol Cell* 18(11):4438–4445.
3. Wykoff DD, O'Shea EK (2001) Phosphate transport and sensing in Saccharomyces cerevisiae. *Genetics* 159:1491–1499.
4. Patton-Vogt JL, Henry SA (1998) GIT1, a gene encoding a novel transporter for glycerophosphoinositol in Saccharomyces cerevisiae. *Genetics* 149:1707–1715.
5. Karandashov V, Bucher M (2005) Symbiotic phosphate transport in arbuscular mycorrhizas. *Trends Plant Sci* 10:22–29.
6. Harrison MJ, Dewbre GR, Liu J (2002) A phosphate transporter from Medicago truncatula involved in the acquisition of phosphate released by arbuscular mycorrhizal fungi. *Plant Cell* 14:2413–2429.
7. Lagerstedt JO, Voss JC, Wieslander A, Persson BL (2004) Structural modeling of dual-affinity purified Pho84 phosphate transporter. *FEBS Lett* 578:262–268.
8. Abramson J, et al. (2003) Structure and mechanism of the lactose permease of Escherichia coli. *Science* 301(5633):610–615.
9. Mueckler M, Makepeace C (2005) Cysteine-scanning mutagenesis and substituted cysteine accessibility analysis of transmembrane segment 4 of the Glut1 glucose transporter. *J Biol Chem* 280:39562–39568.
10. Pascual JM, et al. (2008) Structural signatures and membrane helix 4 in GLUT1: Inferences from human blood-brain glucose transport mutants. *J Biol Chem* 283(24):16732–16742.
11. Voth WP, Jiang YW, Stillman DJ (2003) New 'marker swap' plasmids for converting selectable markers on budding yeast gene disruptions and plasmids. *Yeast* 20(11):985–993.
12. Pernambuco MB, et al. (1996) Glucose-triggered signalling in Saccharomyces cerevisiae: Different requirements for sugar phosphorylation between cells grown on glucose and those grown on non-fermentable carbon sources. *Microbiology* 142:1775–1782.
13. Fiske CH, Subbarow Y (1925) The colourimetric determination of phosphorus. *J Biol Chem* 66:375–400.
14. Van Nuland A, et al. (2006) Ammonium permease-based sensing mechanism for rapid ammonium activation of the protein kinase A pathway in yeast. *Mol Microbiol* 59:1485–1505.
15. Winzeler EA, et al. (1999) Functional characterization of the S. cerevisiae genome by gene deletion and parallel analysis. *Science* 285:901–906.
16. Toda T, et al. (1985) In yeast, RAS proteins are controlling elements of adenylate cyclase. *Cell* 40:27–36.
17. Nikawa J, Cameron S, Toda T, Ferguson KM, Wigler M (1987) Rigorous feedback control of cAMP levels in Saccharomyces cerevisiae. *Genes Dev* 1:931–937.
18. Mbonyi K, van Aelst L, Arguelles JC, Jans AW, Thevelein JM (1990) Glucose-induced hyperaccumulation of cyclic AMP and defective glucose repression in yeast strains with reduced activity of cyclic AMP-dependent protein kinase. *Mol Cell Biol* 10:4518–4523.

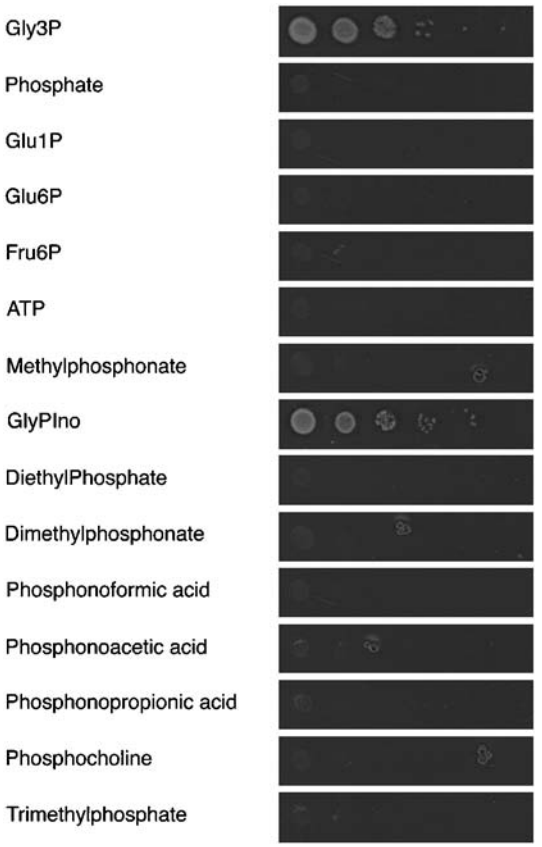

Fig. S1. Growth of the *phoΔnull* strain (*pho84Δ pho87Δ pho89Δ pho90Δ pho91Δ*) with different phosphate-containing compounds or analogues as the sole source of phosphate. The cells were pregrown in SD medium with 10 mM Gly3P as the sole source of phosphate and then spotted in serial tenfold dilutions on plates containing SD medium and 10 mM of the indicated compound as the sole source of phosphate. The plates were incubated for 5 days.

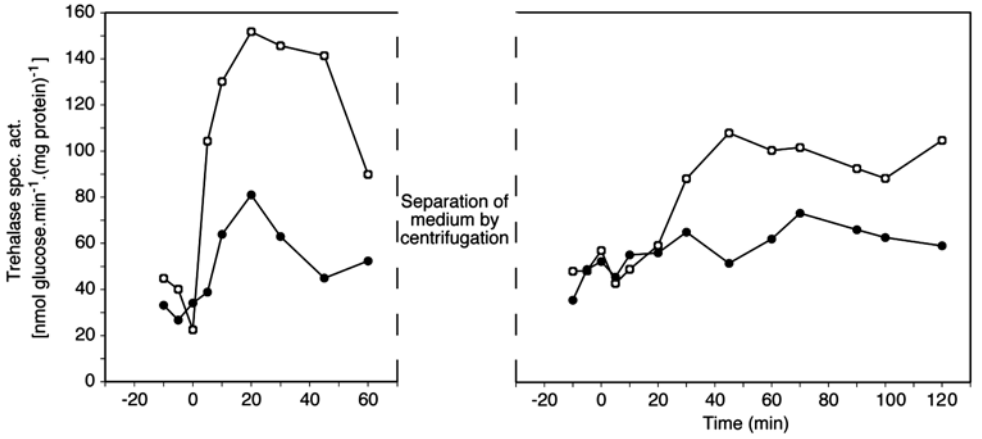

Fig. S2. Activation of the PKA target trehalase after a first addition of Gly3P or phosphate to phosphate-starved cells followed by addition of the remaining supernatant to fresh phosphate-starved cells. First panel: Activation with 0.2 mM phosphate (•) or 10 mM Gly3P (○) added at time zero; second panel: activation with medium obtained after centrifugation of the cells 2 hours after the first activation with 0.2 mM phosphate (•) or 2 hours after the first activation with 10 mM Gly3P (○).

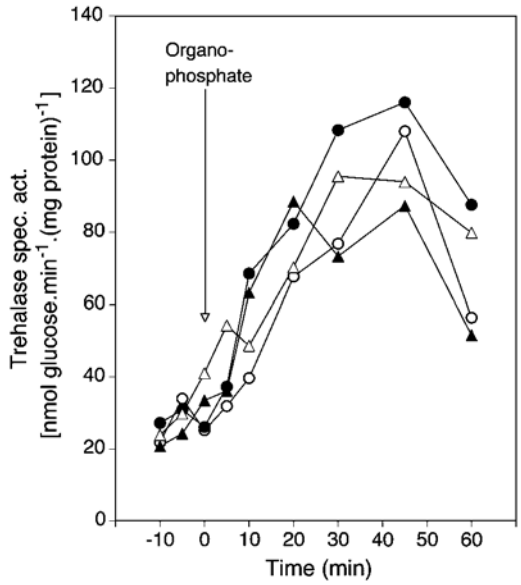

Fig. S3. Activation of the PKA target trehalase after addition of 10 mM of different organophosphate compounds to phosphate-starved cells of the *pho3Δ pho5Δ pho11Δ pho12Δ* strain. Compounds: Gly3P (•), Fructose-6P (○), Glucose-6P (▲), and Glucose-1P (△).

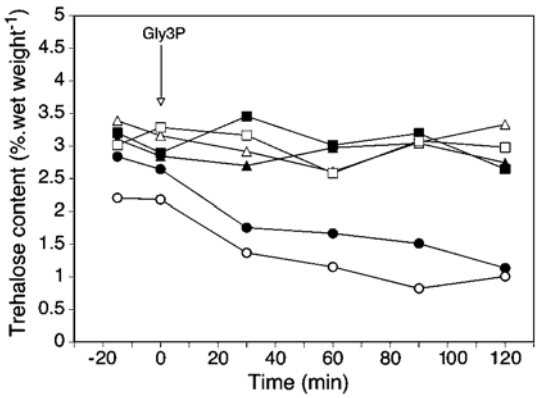

Fig. S4. Only overexpression of *PHO84* sustains Gly3P-induced trehalose mobilization, and it lowers the basal trehalose level. Mobilization of trehalose after addition of Gly3P to phosphate-starved cells of a wild-type strain and a *phoΔnull git1Δ* strain overexpressing only a single phosphate carrier from the *ADH1* promoter. Strains: wild-type (•), *phoΔnull git1Δ* +p*PHO84* (○), +p*PHO87* (▲), +p*PHO90* (△), +p*PHO91* (■), or +p*GIT1* (□).

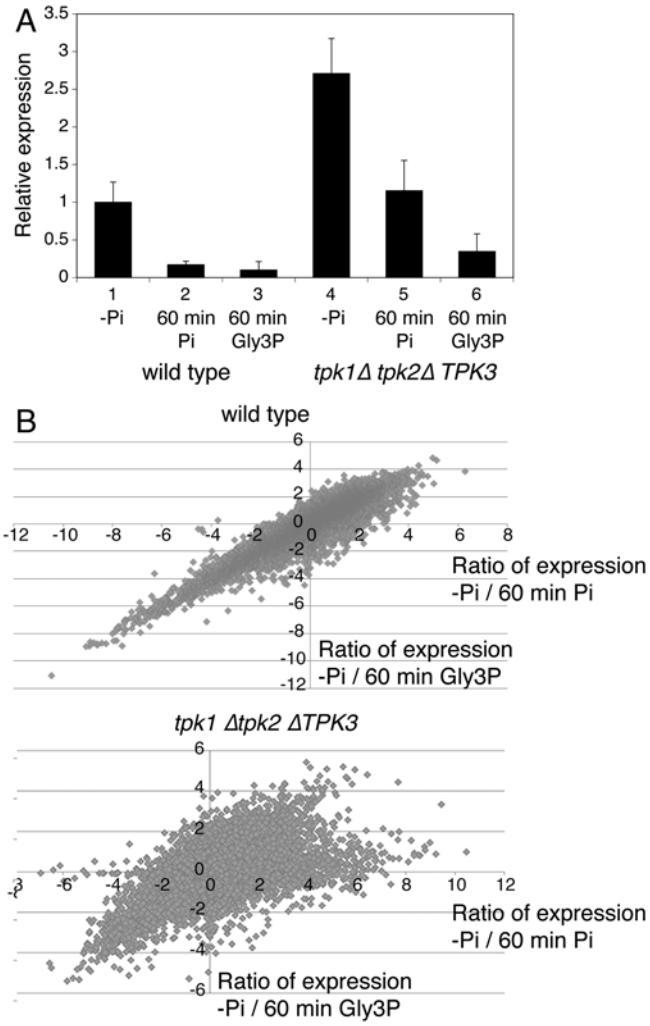

Fig. S5. Phosphate and Gly3P trigger a very similar response in a PKA-dependent manner. (*A*) Expression of the STRE-controlled gene *SSA3* after addition of phosphate or Gly3P for 60 min to cells of the wild-type strain or a strain with reduced PKA activity (*tpk1Δ tpk2Δ TPK3*). (*B*) Microarray analysis of genome-wide gene expression in phosphate-starved cells (control) and in phosphate-starved cells to which phosphate or Gly3P was added for 60 min. The ratio of expression before and after addition of phosphate (*x* axis) is plotted against the ratio of expression before and after addition of Gly3P (*y* axis) for the wild-type strain and the corresponding strain with reduced PKA activity (*tpk1Δ tpk2Δ TPK3*).

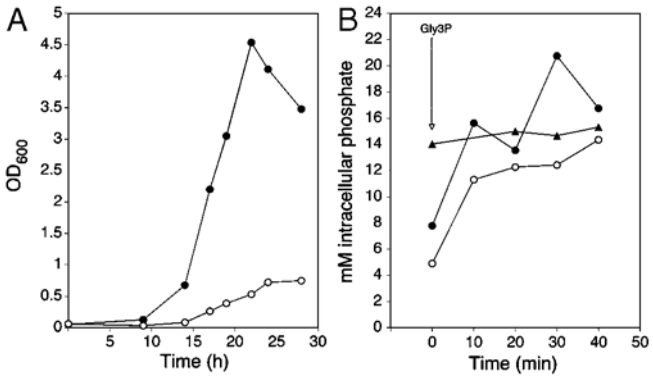

Fig. S6. Uptake of Gly3P occurs through Git1 and Pho91 as measured by growth recovery and intracellular phosphate levels. (*A*) Growth recovery of phosphate-starved cells after addition of Gly3P. Strains: *pho3Δ pho5Δ* (•) and *git1Δ pho91Δ pho3Δ pho5Δ* (○). (*B*) Intracellular phosphate level after addition of 10 mM Gly3P to cells grown in phosphate-limited conditions. Strains: wild-type (•), *pho3Δ pho5Δ* (○), and *git1Δ pho91Δ pho3Δ pho5Δ* (▲).

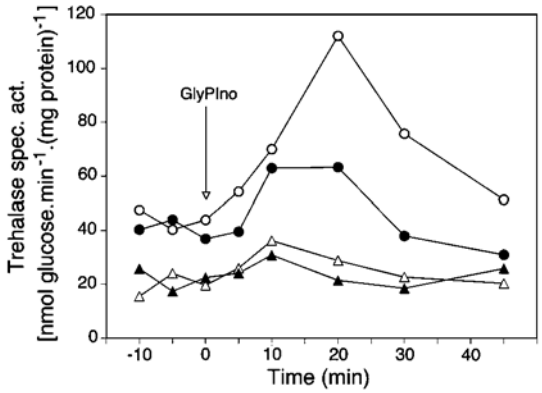

Fig. S7. Activation of the PKA target trehalase after addition of GlyPIno to phosphate-starved cells. Addition of 0.1 (•) or 0.5 mM (○) GlyPIno to cells of the *git1Δ pho3Δ pho5Δ* strain and 0.1 (▲) or 0.5 mM (△) GlyPIno to cells of the *pho84Δ pho3Δ pho5Δ* strain.

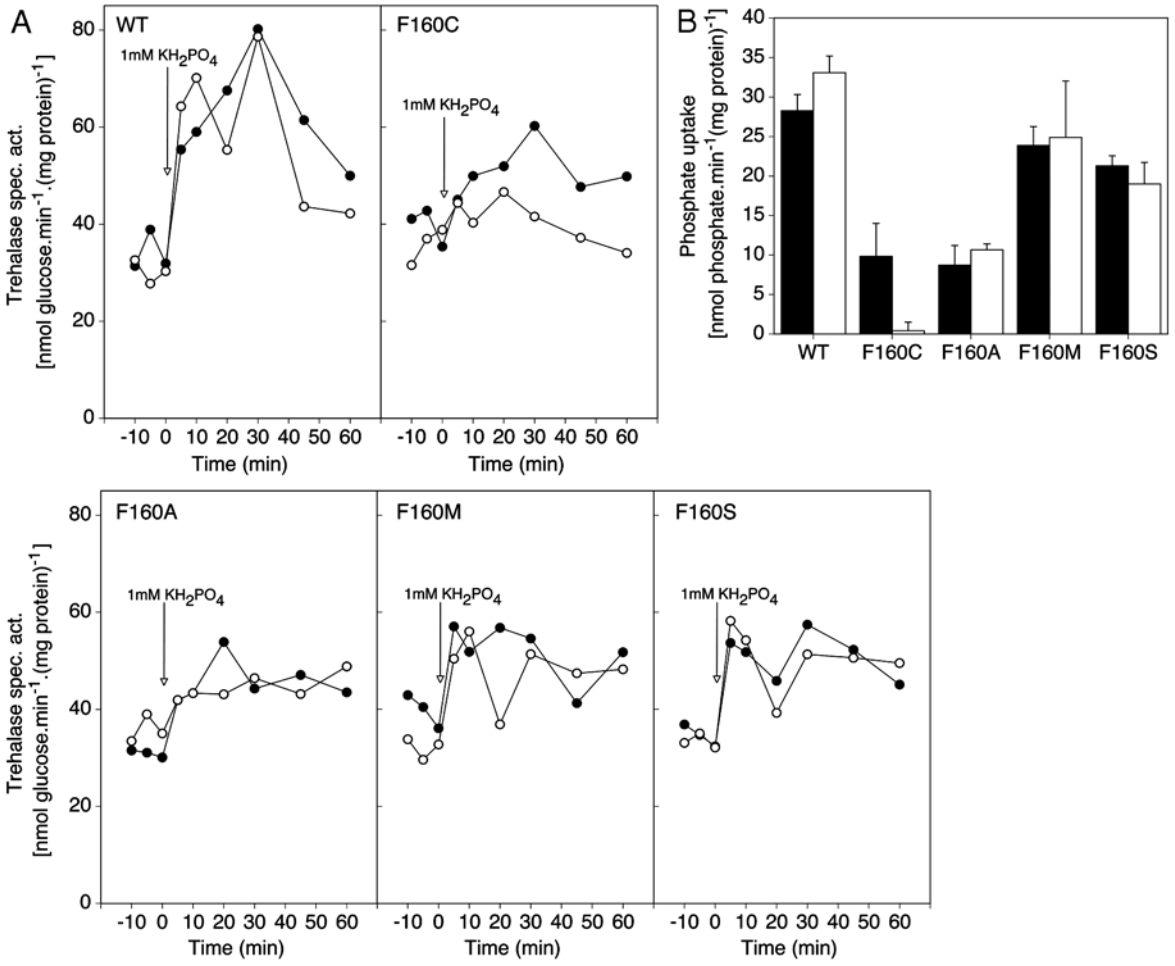

Fig. S8. Activation of the PKA target trehalase and transport of phosphate in phosphate-starved cells of strains expressing a Pho84^{F160} mutant allele, with or without pretreatment with MTSEA. (*A*) Activity of trehalase after addition of 1 mM phosphate without (•) and with (○) preaddition of 10 mM MTSEA, in cells expressing a Pho84^{F160} mutant allele as indicated. (*B*) Transport of 1 mM phosphate in cells expressing a Pho84^{F160} mutant allele as indicated, without (black bars) and with (white bars) preaddition of 10 mM MTSEA.

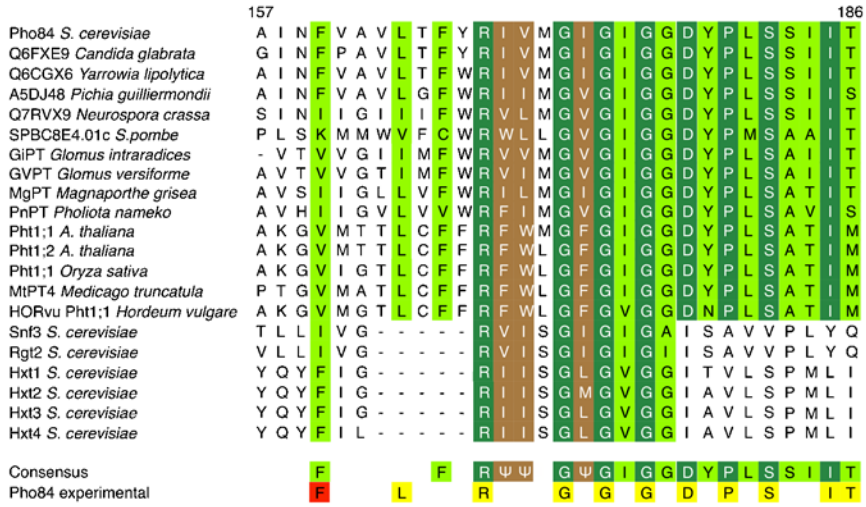

Fig. S9. Alignment of TMD IV of Pho84 with the same domain in other phosphate carriers, in the glucose sensors Snf3 and Rgt2, and in the Hxt glucose carriers. Color coding: dark green, strictly conserved residues; light green: residues with only conservative substitutions; brown: hydrophobic residues. The residues in Pho84 that were experimentally shown to be important for transport and signaling are indicated at the bottom with the following color coding: yellow, strongly reduced or completely abolished transport and signaling; red, partially reduced transport and signaling in the cysteine substitution protein and deficient transport and signaling after preaddition of 10 mM MTSEA.

Table S1. List of yeast strains used in this study

Strain	Relevant genotype	Reference
Strains isogenic to EY57		
EY57	*MATa ade2-1 trp1-1 can1-100 leu2-3,112 his3-11,15 ura3*	(3)
EY914	EY57 *MAT pho84::HIS3 pho3::LEU2*	(3)
EY915	EY57 *MAT pho3::LEU2*	(3)
EY917(*phoΔnull*)	EY57 *MAT pho84::HIS3 pho87::CgHIS3 pho89::CgHIS3 pho90::CgHIS3 pho91::KlURA3*	(3)
YP100	EY917 *git1::KanMX4 pGAL1-PHO84* (EB1280)	This work
YP101	EY917 *git1::KanMX4 pADH1-GIT1* (EB1374)	This work
YP102	EY917 *git1::KanMX4 pADH1-PHO84* (EB1368)	This work
YP103	EY917 *git1::KanMX4 pADH1-PHO87* (EB1247)	This work
YP104	EY917 *git1::KanMX4 pADH1-PHO90* (YP1314)	This work
YP105	EY917 *git1::KanMX4 pADH1-PHO91* (YP1315)	This work
YP106	EY917 *pho5::KanMX4 git1::KanMX4::LEU2*	This work
YP107	EY915 *MAT pho84::HIS3 pho5::KanMX4*	This work
YP108	EY915 *MAT pho5::KanMX4*	This work
YP109	EY915 *MAT pho5::KanMX4 git1::TRP1*	This work
YP110	EY915 *MAT pho5::KanMX4 pho91::KlURA3*	This work
YP111	EY915 *MAT pho5::KanMX4 git1::TRP1 pho91::KlURA3*	This work
Strains isogenic to S288c		
Y15815	*MAT leu2 lys2 ura3 git1::KanMX4*	(15)
Y13232	*MAT leu2 lys2 ura3 pho5::KanMX4*	(15)
Strains isogenic to SP1		
SP1	*MATa leu2 his3 trp1 ade8 can1 ura3*	(16)
S7-7A	SP1 *tpk2::HIS3 tpk3::TRP1*	(17)
JT2119	SP1 *tpk1::URA3 tpk3::TRP1*	(18)
JT2117	SP1 *tpk1::URA3 tpk2::HIS31*	(18)
S18-1D	SP1 $tpk1^{w1}$ *tpk2::HIS3 tpk3::TRP1*	(17)
RS13-58A-1	SP1 $tpk1^{w1}$ *tpk2::HIS3 tpk3::TRP1 bcy1::LEU2*	(17)
S15-5B	SP1 *tpk1::URA3* $tpk2^{w1}$ *tpk3::TRP1*	(17)
RS13-7C-1	SP1 *tpk1::URA3* $tpk2^{w1}$ *tpk3::TRP1 bcy1::LEU2*	(17)
S22-5D	SP1 *tpk1::URA3 tpk2::HIS3* $tpk3^{w1}$	(17)
RTF3.1-1	SP1 *tpk1::URA3 tpk2::HIS3* $tpk3^{w1}$ *bcy1::LEU2*	(17)